10% Component Efficiency of Fully Integrated and Oxide Embedded Photonic Crystal Cavity

Maakbul H. K. Anik, Heijun Jeong, Masudur Rahim, Yahui Xiao, and Tingyi Gu
Electrical and Computer Engineering, University of Delaware, Newark, DE 19711 USA
Author e-mail address: tingyigu@udel.edu.

Abstract: We demonstrated low insertion loss fully integrated photonic crystal cavity with on-chip metalens coupling, with experimentally measured total quality factor of 10^4.

1. Introduction

The deployment of a photonic crystal (PhC) cavity is highly advantageous in various fields such as coherent electron-photon interaction, optical filters, sensing, and quantum information processing [1,2]. Its ability to achieve strong light confinement within a small mode volume, quantified as the quality factor (Q) versus modal volume size (V), enhances the light-matter interaction for energy efficient optoelectronics and low threshold nonlinear optic response. In traditional PhC systems, single-mode waveguides (WG) are typically employed to establish a connection between the individual components. In conventional photonic crystal cavity design, top oxide removal and undercut are typically required for enhancing Q/V. This poses difficulties for subsequent postprocessing steps and limit the feasibility of large-scale integration [3]. A fully embedded PhC cavity has been experimentally demonstrated through the wafer-scale foundry runs, but the insertion loss remains high [4].

This study presents a new approach to enhance the efficiency of light coupling in a cavity area by integrating a low loss dielectric metalens with a PhC cavity in which the proposed design incorporates a coupler angle of 60^0, which facilitates the increased coupling of light in the cavity region as it passes through the metalens. The mechanical robustness of this fully integrated PhC L3 (three missing holes) cavity is enhanced by the absence of WG and the direct coupling between metalens and the PhC resonator through particle swarm optimization (PSO) of certain parameters of the resonator, which results in a Q/V greater than 10^{10} cm^{-3} holding a great potential for various applications, including biosensors, nonlinear optics, and hybrid lasers.

2. Design and Numerical Analysis

The PhC L3 cavity resonator and dielectric metalens are positioned on the same layer on the SOI substrate, which consists of a 250 nm Si slab over 3 μm thick SiO_2 with a 7.6 μm wide metalens in the y-direction illustrated in Fig. 1(a) as a 2D top view. The 1D-dielectric metalens with a focus length (f) of 15 μm is employed to manipulate the wavefront and introduces a phase shift that varies with position in the y-direction for TE-polarized incident light propagating along the x-direction [5]. The airholes in the PhC L3 (missing three airholes) cavity structure have a lattice constant of a = 0.393 μm and a radius of 0.33a μm. The PhC structure exhibits two distinct categories of airholes that demonstrate high sensitivity to Q/V and peak transmission. These categories include end holes, which are situated at both ends of the L3 cavity, and edge holes, which are positioned on outer sides of the L3 cavity where light enters and exits the L3 line. The incident light is directed towards the PhC L3 cavity in order to stimulate a fundamental

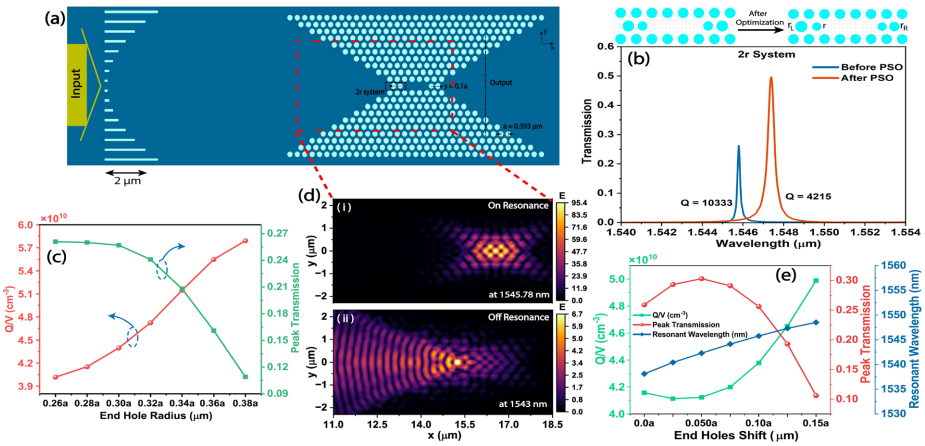

Fig. 1 (a) 2D top view of the PhC-metalens system. (b) Comparison of transmission spectra before and after applying PSO optimization. Radii of end and edge holes along with shifting of end holes are the design parameters where PSO was used employing total around 1800 simulations. After PSO, r = 0.285a, r_L = 0.381a, r_R = 0.321a, left end hole s = 0.0a and right end hole s = 0.214a μm. (c) Changes in Q/V and peak transmission due to end hole radius variation. (d) E-field intensity profile at on and off resonances. (e) Q/V, transmission peak and resonant wavelength variations as a function of end holes shifting.

resonance mode with a wavelength of about 1.55 μm. Prior to PSO, the radii of the end and edge holes were 0.30a μm and 0.357a μm, respectively, with the end holes shifted by s = 0.10a μm forming additional space in the cavity region for light confinement. The optimal design parameters in terms of maximum transmission were determined by running a PSO by varying a few factors that were sensitive to Q/V and peak transmission of the design, such as end and edge hole radii and end hole shifting. Fig. 1(b) exhibits a comparison of transmission spectra before and after optimization, with the transmission peak increasing to 0.5 after optimization from 0.256 initially. Prior to optimization, the Q-factor was computed to be 10333; however, following optimization, it is estimated to be around 4215. Fig. 1(c) depicts the variations in peak transmission and Q/V as the radius of the end holes is altered in which the modal volume is computed using this $V = \frac{\int \epsilon(r)|E(r)|^2 dV}{\max[\epsilon(r)|E(r)|^2}$ equation [6]. While the Q/V grows approximately linearly with the increase in end hole radius, the transmission peak diminishes exponentially as the end hole radius increases. The electric field distribution is illustrated in Figure 1(d) at 1545.78 nm (i) and 1543 nm (ii), the locations where cavity resonance and back reflection of light take place, respectively. The alteration of the end holes' position to enlarge the cavity area leads to notable changes in the Q/V ratio, transmission peak, and resonant wavelength, as seen in Fig. 1(e). In order to achieve enhanced light confinement and a high Q-factor, it is imperative to disregard any sudden variations in the electric field occurring near the borders of the cavity. When the end holes of the cavity are shifted towards the edge holes, the phase-mismatch reduces the amount of Bragg reflection which in turn, allows for increased penetration of light into the cavity. We have utilized the 2.5D varFDTD-based Ansys Lumerical simulation tool in order to get the findings that are displayed in Fig. 1.

3. Device Fabrication and Measurement

The on-chip metalens was produced on a SOI device including a 250 nm-thick layer of silicon on top of a 3μm-thick layer of silicon dioxide. The design components, such as PhC, metalens, and grating couplers, were fabricated using CSAR 6200.09 positive resist. The fabrication process involved the utilization of a Vistec EBPG5200 electron beam lithography equipment, followed by resist development and a single step dry etch method. A silicon dioxide protective layer with a thickness of 900 nm is applied onto the device layer using plasma-enhanced chemical vapor deposition (PECVD). The metalens-PhC cavity's scanning electron microscopy (SEM) image is displayed in Fig. 2(a). The experimentally measured transmission curve for the optimized device is shown in Fig. 2(b), with a peak transmission of 0.1 in linear scale.

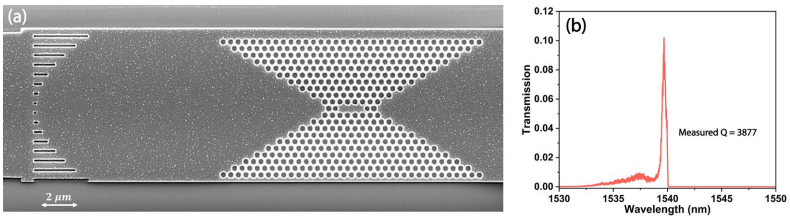

Fig. 2 (a) SEM image of the metalens-PhC cavity system. (b) Experimentally measured transmission curve of the optimized device.

In conclusion, this study first presents a numerical demonstration of a metalens-PhC cavity design that enhances light coupling via optimization of specific device parameters. Variations in Q/V resulting from deviations in parameters such as the radius and shifting of the cavity's end holes are also described in this work. Finally, the metalens-PhC cavity device has been fabricated, and the transmission curve of the optimized device, as determined through simulation, is measured.

References

[1] S. Noda, M. Fujita, and T. Asano, "Spontaneous-emission control by photonic crystals and nanocavities," Nat. Photonics, vol. 1, no. 8, Art. no. 8, Aug. 2007.

[2] P. Lalanne, C. Sauvan, and J. p. Hugonin, "Photon confinement in photonic crystal nanocavities," Laser Photonics Rev., vol. 2, no. 6, pp. 514–526, 2008.

[3] Y. Xiao, Z. Wang, F. Wang, H. Lee, T. Kananen, and T. Gu, "Engineering the light coupling between metalens and photonic crystal resonators for robust on-chip microsystems," J. Opt. Microsyst., vol. 1, no. 2, p. 024001, Mar. 2021.

[4] D. Dodane, J. Bourderionnet, S. Combrié, and A. de Rossi, "Fully embedded photonic crystal cavity with Q=0.6 million fabricated within a full-process CMOS multiproject wafer," Opt. Express, vol. 26, no. 16, pp. 20868–20877, Aug. 2018.

[5] Z. Wang, T. Li, A. Soman, D. Mao, T. Kananen, and T. Gu, "On-chip wavefront shaping with dielectric metasurface," Nat. Commun., vol. 10, no. 1, Art. no. 1, Aug. 2019.

[6] S. Hu et al., "Experimental realization of deep-subwavelength confinement in dielectric optical resonators," Sci. Adv., vol. 4, no. 8, p. eaat2355, Aug. 2018.